Influence of the softness of the repulsive core interaction on cluster melting

C. Rey, J. García-Rodeja, and L. J. Gallego

Departamento de Física de la Materia Condensada, Facultad de Física, Universidad de Santiago de Compostela,
E-15706 Santiago de Compostela, Spain

M. J. Grimson

Department of Physics, University of Auckland, Private Bag 92019, Auckland, New Zealand
(Received 12 September 1997)

The influence of the softness of the repulsive core of the pair interaction on the melting behavior of small clusters was studied by molecular-dynamics simulation of clusters in which particles interact through pairwise additive, inverse-power-based potentials. The potentials used had minima of the same depth and position and were identical beyond the minimum, differing only in the softness of the repulsive core. Core softness was found to favor a two-step cluster melting process. [S1063-651X(98)05804-8]

I. INTRODUCTION

Although considerable effort has been devoted to investigating by molecular dynamics (MD) and Monte Carlo (MC) simulations the melting behavior of clusters containing a small number of atoms (see, e.g., Refs. [1,2] and those cited therein), this is a phenomenon that, in some respects, still remains challenging. In transition-metal clusters of sizes allowing the formation of complete icosahedra or polyicosahedra plus an extra atom (e.g., clusters with $N=14$ and $N=20$ atoms) the existence of a premelting phenomenon (local melting of the cluster due to the destabilization of the extra atom) has been predicted using Gupta-like and embedded-atom potentials [3,4]. Because this effect had not been observed among Lennard-Jones (LJ) clusters, the occurrence of premelting was attributed to the many-body character of the metallic interaction.

A different phenomenon is that of surface melting, an effect recognized by Briant and Burton [5] and on which a number of workers have focused their attention recently. Cheng and Berry [6] have combined analytical and MD methods to study the dynamic aspects of surface melting in Ar_N clusters with LJ interaction potentials ($N=40–147$) and Cu_{55} clusters with embedded-atom potentials. More recently, Calvo and Labastie [7] have analyzed, from both the thermodynamic and structural points of view, the melting characteristics of double-icosahedron-based LJ clusters up to a size of $N=34$ atoms, showing that for several sizes (and particularly for $N=34$) the cluster surface melts before the core, which remains in a solidlike state until complete melting. The possibility of surface melting prior to full melting has also been investigated by Krissinel and Jellinek [8] in Ni_{13}, Al_{13}, and some mixed 13-atom Ni-Al clusters using a Gupta-like potential for MD simulations. It was found that a two-step process occurs in the solid-to-liquid transition for Ni_{13} and Al_{13}: The first step corresponds to isomerizations involving only surface atoms but without giving rise to a proper surface-melted stage and the second to isomerizations that involve the central atom.

MC simulations have been carried out recently to analyze the influence of the range of the attractive interaction on the phase behavior of small clusters of particles interacting via hard-core Yukawa (HCY) potentials [9]. These calculations showed that the existence and extent of a liquidlike cluster phase depends on the range of the attractive Yukawa interaction. Decreasing the range of the potential destabilizes the liquidlike phase, with the result that cluster sublimation takes place before liquidlike behavior begins. A similar conclusion was also arrived at by Doye and Wales [10] using a Morse potential. By comparing the results for HCY clusters with those of Hagen and Frenkel [11] for bulk HCY fluids, it was shown that the shortest tail range allowing a liquid phase in the cluster system is significantly longer than for bulk matter. This means that, in general, the nonexistence of liquidlike cluster states is not necessarily incompatible with the existence of a stable bulk liquid phase. The results of Rey, Gallego, and Alonso [12] and Cheng, Klein, and Caccamo [13] show that fullerene (C_{60}) may be a case in point.

As far as we know, no similar detailed studies have hitherto been carried out to investigate the influence of the shape of the potential in the core region. This paper reports the results of our research in this area. Specifically, we constructed a series of pair interaction potentials differing only in their shape in the core region (the depth and position of the minimum were the same in all and all were identical beyond the minimum) and we carried out MD simulations to investigate the melting of clusters of particles interacting via each potential in a pairwise additive fashion. We found that these clusters exhibited two-step melting if the core repulsion was soft enough, which suggests that the two-step processes observed in simulations of metal clusters may probably also be attributed to the softness of the cores of the potentials used rather than to many-body effects.

In Sec. II we introduce a scheme to analyze the effects of core softness on cluster melting behavior and give some details of the computational procedure used in this work. In Sec. III we present and discuss our results. Finally, the main conclusions of our study are summarized in Sec. IV.

II. MODEL POTENTIAL AND SIMULATION DETAILS

As indicated above, we wish to study how the melting characteristics of a cluster of N particles interacting through

a pairwise potential $\Phi(r)$ depend on the softness of the core potential. To do so, we construct a model for $\Phi(r)$ that allows the range of $\Phi(r)$, and the location and depth of its minimum, to be held constant while the softness of the core is varied.

Consider a general m-n inverse power potential of the form

$$\varphi(r;m,n) = \alpha\epsilon\left[\left(\frac{\gamma\sigma}{r}\right)^m - \left(\frac{\gamma\sigma}{r}\right)^n\right]. \qquad (1)$$

The minimum of $\varphi(r;m,n)$ is located at r_0, defined by

$$\left(\frac{\partial\varphi(r;m,n)}{\partial r}\right)_{r=r_0} = 0, \qquad (2)$$

which gives

$$r_0 = \sigma\gamma\left(\frac{m}{n}\right)^{1/(m-n)}. \qquad (3)$$

Thus

$$\varphi(r_0;m,n) = \alpha\epsilon\left(\frac{n}{m}\right)^{n/(m-n)}\left(\frac{n}{m}-1\right). \qquad (4)$$

If we now require the location and depth of the potential minimum for all m and n to be identical to the values for the familiar 12-6 LJ potential, namely, $r_0 = 2^{1/6}\sigma$ and $\varphi(r_0;m,n) = -\epsilon$, then the coefficients α and γ of the potential $\varphi(r;m,n)$ will be given by

$$\frac{1}{\alpha} = \left(1-\frac{n}{m}\right)\left(\frac{n}{m}\right)^{n/(m-n)} \qquad (5)$$

and

$$\gamma = 2^{1/6}\left(\frac{n}{m}\right)^{1/(m-n)}, \qquad (6)$$

respectively. For $m=12$ and $n=6$, we have $\alpha=4$ and $\gamma=1$ and thus recover the familiar results for the 12-6 LJ interaction potential. Varying m and n allows the softness of the core of $\varphi(r;m,n)$ to be varied, but not without altering the range of the potential.

To see how the range of the model potential can be held fixed, as well as its minimum, while varying the softness of the core, consider the Weeks-Chandler-Andersen (WCA) scheme [14] for splitting an interaction potential $\varphi(r)$ into reference and perturbation components:

$$\varphi(r) = \varphi_0(r) + \varphi_1(r), \qquad (7)$$

where the short-range repulsive reference potential $\varphi_0(r)$ is defined by

$$\varphi_0(r) = [\varphi(r)-\varphi(r_0)]\theta(r-r_0), \qquad (8)$$

the long-range attractive perturbation potential $\varphi_1(r)$ is given by

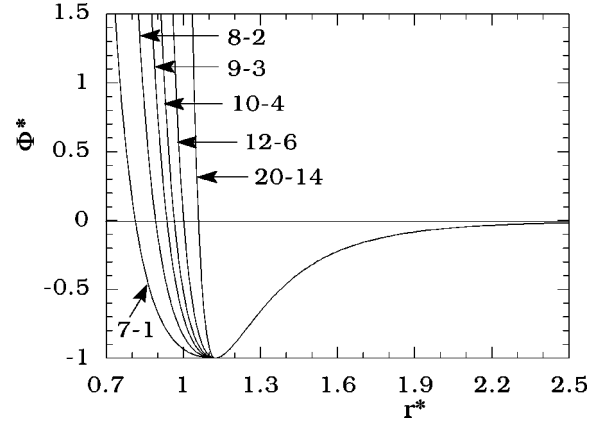$$\varphi_1(r) = \varphi(r)\theta(r_0-r) + \varphi(r_0)\theta(r-r_0), \qquad (9)$$

FIG. 1. Pair potential $\Phi(r;m_0,n_0)$ for several values of m_0-n_0.

and $\theta(x)$ is the Heaviside step function [$\theta(x)=1$ if $x<0$ and $\theta(x)=0$ if $x>0$]. In constructing our model potential $\Phi(r)$, we shall utilize the general m-n interaction potentials $\varphi(r;m,n)$ introduced above together with the WCA scheme for splitting the interaction potential. This allows different choices of m and n for the reference and perturbation potentials and thereby an extra degree of control. Our model potential $\Phi(r)$ is chosen such that

$$\Phi(r) \equiv \Phi(r;m_0,n_0,m_1,n_1) = \varphi_0(r;m_0,n_0) + \varphi_1(r;m_1,n_1).$$

$$(10)$$

We note that the WCA scheme ensures that the composite pair potential and its first derivative are continuous for all r, even when $m_0 \neq m_1$ and $n_0 \neq n_1$. To ensure that the range of the potential $\Phi(r;m_0,n_0,m_1,n_1)$ is the same for all systems, we shall choose m_1 and n_1 (and hence the long-range region of the potential) to be the same for all systems under consideration. For simplicity, we take $m_1=12$ and $n_1=6$. Then the long-range part of the potential, $\Phi(r)$ for $r>r_0$, is identical to the familiar 12-6 LJ potential. Henceforth, we shall denote the potential $\Phi(r;m_0,n_0,m_1=12,n_1=6)$ simply as $\Phi(r;m_0,n_0)$ and refer to it as the m_0-n_0 potential. Figure 1 shows the form of this potential for different values of m_0 and n_0.

We have investigated by means of MD simulations the melting behavior of clusters with $N=13$ particles interacting through the model potential $\Phi(r;m_0,n_0)$ described above for all the values of m_0 and n_0 indicated in Fig. 1. The 13-particle cluster is a paradigmatic system for studies on LJ clusters (see, e.g., Refs. [2,15,16]) since the ground-state icosahedral structure is very stable and thus offers an appropriate system for analyzing the rigid (solidlike) to nonrigid (liquidlike) transition. However, although our attention was primarily focused on the 13-particle cluster, some calculations were also made for clusters with $N=14$ particles in order to highlight some aspects of the premelting phenomenon.

Computations were carried out using ϵ, σ, and $\tau=(M\sigma^2/\epsilon)^{1/2}$, where M is the particle mass, as units of energy, distance, and time, respectively. Quantities expressed in these reduced units will be indicated by an asterisk. MD simulations were performed using the velocity Verlet algorithm [17] with a time step of 5×10^{-3}, which
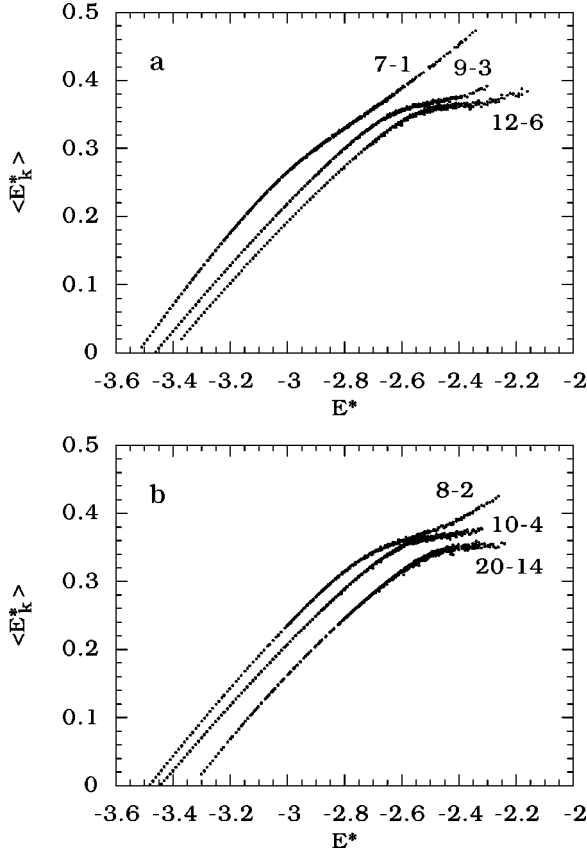
FIG. 2. Caloric curves showing the mean kinetic energy per particle as a function of the total energy per particle for 13-particle clusters with pair potentials $\Phi(r;m_0,n_0)$.

guarantees conservation of the total cluster energy to within 0.01%. The melting behavior of the different clusters was investigated by gradually heating nonrotating, nontranslating structures in a stepwise manner to obtain the caloric curves (see, e.g., Ref. [18]). For each heating step, the system was allowed to propagate over 101×10^4 time steps. The first 10^4 time steps allowed for equilibration of the cluster, while the remaining 10^6 time steps were used to obtain the state point on the caloric curve by averaging the kinetic energy E_k and potential energy U. The total energy E_k+U is denoted by E. In general, for each state point this process was repeated twice. However, in the transition region, where large thermodynamic fluctuations occur, between four and ten repetitions were performed. In the course of the MD simulations the relative root-mean-squared (rms) pair separation fluctuation δ and the specific heat C were calculated using the expressions [19]

$$\delta = \frac{2}{N(N-1)}\sum_{i<j}\frac{(\langle r_{ij}^2\rangle - \langle r_{ij}\rangle^2)^{1/2}}{\langle r_{ij}\rangle} \tag{11}$$

and

$$C = \frac{k}{N}\left[1 - \left(1 - \frac{2}{3N-6}\right)\langle E_k\rangle\langle E_k^{-1}\rangle\right]^{-1}, \tag{12}$$
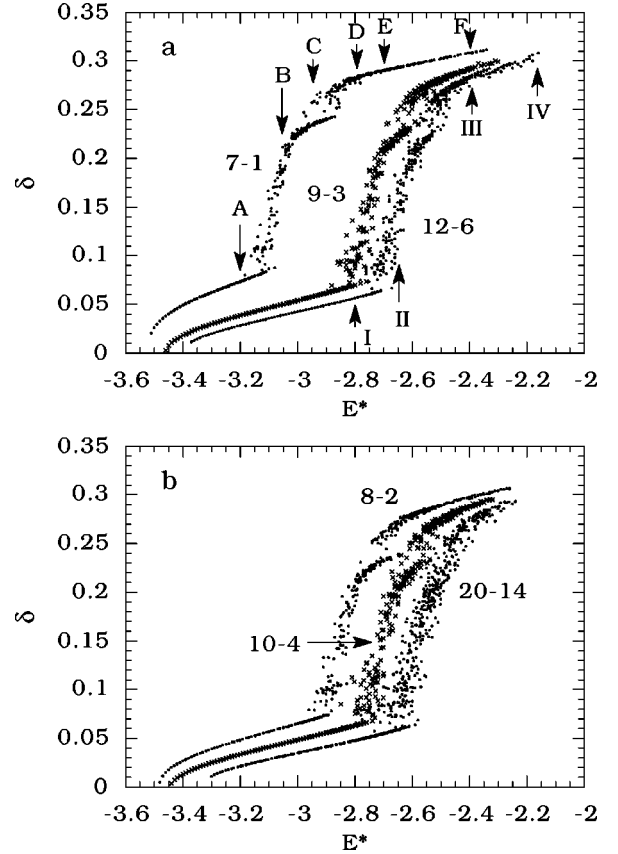

FIG. 3. The rms pair separation fluctuation as a function of the total energy per particle $\delta(E^*)$ for 13-particle clusters with pair potentials $\Phi(r;m_0,n_0)$. The energies indicated by arrows are as follows: A, -3.2; B, -3.05; C, -2.95; D, -2.8; E, -2.7; F, -2.4; I, -2.8; II, -2.65; III, -2.4, and IV, -2.16.

where r_{ij} is the distance between particles i and j, k is the Boltzmann constant, and angular brackets denote averages over an entire run after equilibration.

III. RESULTS AND DISCUSSION

Figures 2–4 show the computed caloric ($\langle E_k^*\rangle(E^*)$), $\delta(E^*)$, and specific-heat $[(C^*(E^*)]$ curves for the 13-particle cluster with interaction potential $\Phi(r;m_0,n_0)$ for the values of m_0 and n_0 given in Fig. 1. The results for $m_0=12$ and $n_0=6$, which correspond to the familiar 13-particle LJ cluster and act as a point of reference, are in good agreement with those reported elsewhere [2,15,16]. In all of the cases studied in this paper, the 13-particle cluster undergoes a solidlike to liquidlike transition, which is indicated by the changes in the slope of the caloric curves, abrupt increases in the $\delta(E^*)$ graphs, and peaks in the specific heats. For the softer 7-1, 8-2, 9-3, and 10-4 potentials, there are clearly two abrupt increases in $\delta(E^*)$; for the harder 12-6 and 20-14 potentials, the second rise is less clearly defined. By careful examination of the cluster structures during the simulations performed with the 7-1 potential, we found that the first abrupt change in $\delta(E^*)$ corresponds to the onset of frequent isomerizations involving only the surface atoms, while the second abrupt change in $\delta(E^*)$ corresponds to the onset of frequent isomerizations that involve the central atom.
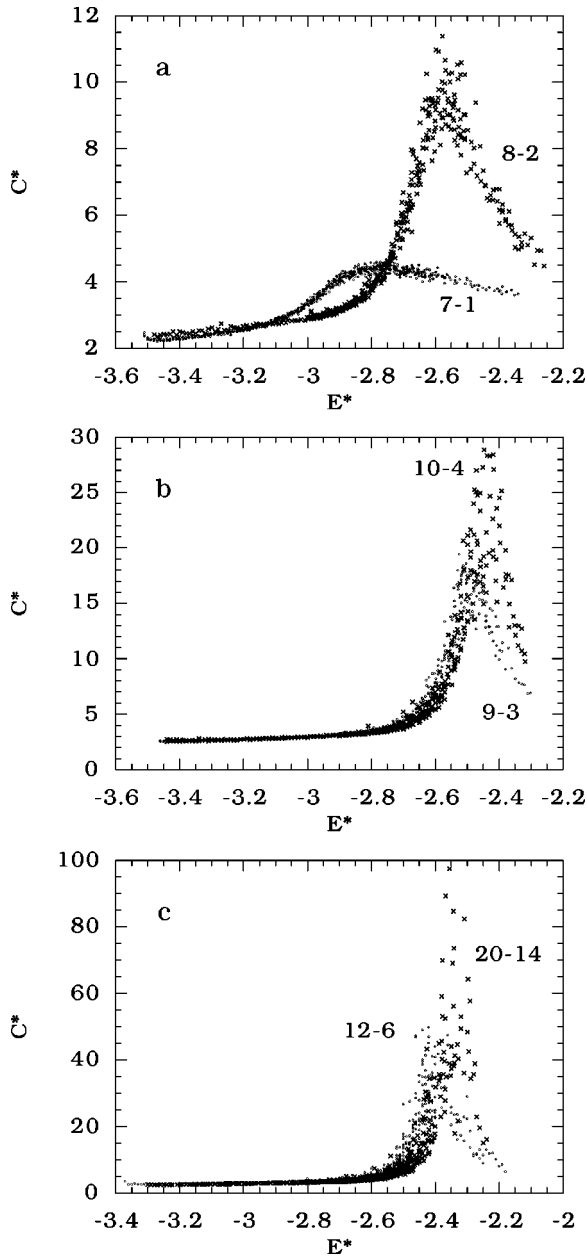
FIG. 4. Specific heat per particle as a function of the total energy per particle for 13-particle clusters with pair potentials $\Phi(r; m_0, n_0)$.

Figure 4 shows that only a single peak appears in each specific-heat curve. Although these peaks are very broad for the softer potentials, the apex corresponds in all cases to an energy (the ''melting energy'') that is slightly higher than that of the second abrupt increase in $\delta(E^*)$. Melting requires the participation of all atoms (including the central one) in diffusive motion. The absence of any separate peak in $C^*(E^*)$ at an energy between those of the two abrupt changes in δ is presumably because in this work the isomerizations involving only surface atoms did not constitute a well-defined surface-melted state.

MD simulations carried out by Jellinek, Beck, and Berry [15] for the 13-atom LJ cluster have shown that the short-time-averaged potential energy has a bimodal distribution at total energies between those at which the long-time-averaged
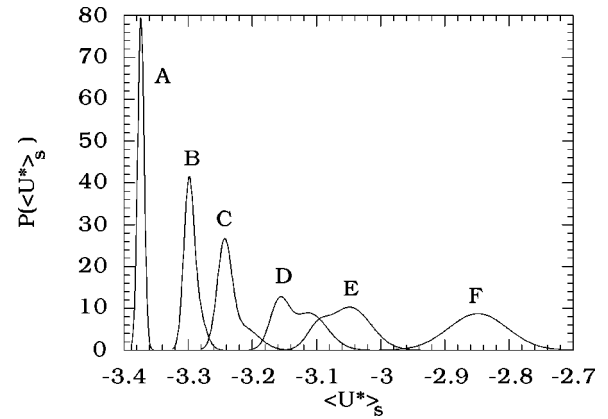

FIG. 5. Distribution of the short-time (250 time step) average of the potential energy per particle for a 13-particle cluster with a 7-1 pair potential for total energies per particle indicated by the arrows labeled $A-F$ in Fig. 3(a). $P(\langle U^*\rangle_s)$ is the normalized probability density. Each curve is the best fit to the data of a sum of two Gaussians, except for curves A and F, which are the best fits of single Gaussians.

caloric curve changes slope. We have observed this bimodal behavior in the 13-particle cluster for all the potentials considered in this paper. By way of illustration, the results for the softest (7-1) potential are shown in Fig. 5, where $\langle\ \rangle_s$ denotes a short-time average. It should be pointed out that such bimodality does not necessarily imply that at certain total energies the cluster can fluctuate between well-defined phases (or, invoking the ergodic hypothesis, that there is a range of total energies in which a microcanonical ensemble of clusters is a mixture of rigid solidlike and nonrigid liquid-like forms). For fluctuation between phases, the cluster must remain in each phase long enough to allow its proper characterization. To clarify this point, in Figs. 6 and 7 we show the time course of the short-time (250-step) averages of the potential energies of 13-particle clusters with 12-6 and 7-1 potentials for the total energies indicated by arrows in Fig. 3. In the case of the 12-6 potential (which does allow fluctuation between phases, as we shall see), one can distinguish the following situations. At low total energy [Fig. 6(I)], in the solidlike region, the short-time-averaged potential energy is
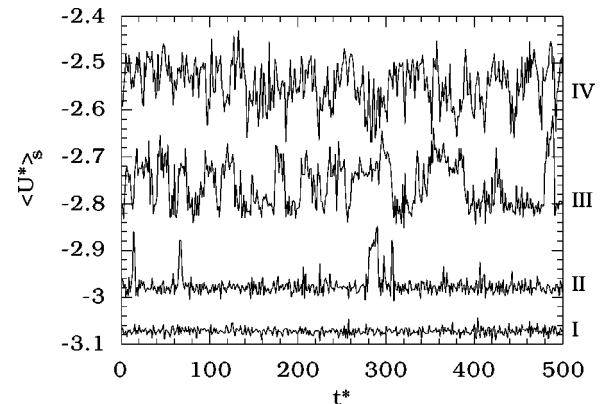

FIG. 6. Short-time averages of the potential energy as a function of time for a 13-particle cluster with a 12-6 pair potential. The total energy per particle for each curve is indicated by the corresponding arrow in Fig. 3(a).
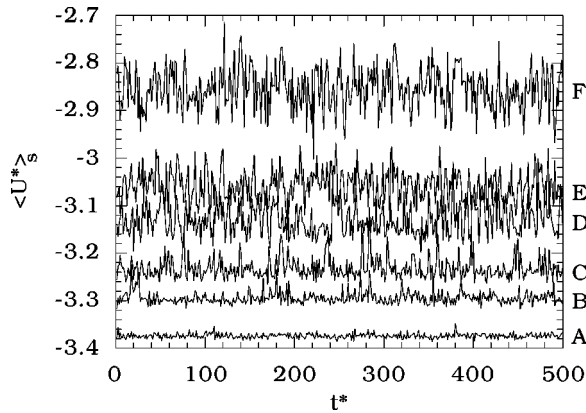
FIG. 7. Short-time averages of the potential energy as a function of time for a 13-particle cluster with a 7-1 pair potential. The total energy per particle for each curve is indicated by the corresponding arrow in Fig. 3(a).

FIG. 8. Caloric curve (crosses) and $\delta(E^*)$ (dots) for a 14-particle cluster with a 7-1 pair potential.

essentially constant. At higher energies [Fig. 6(II)], there are occasional peaks, some of which correspond to isomerizations involving only surface atoms. In the region of bimodality (i.e., at total energies between about -2.64 and -2.25; see Ref. [15]) $\langle U^* \rangle_s$ fluctuates between two levels corresponding to two distinct cluster forms: a rigid, solidlike form of lower potential energy and a nonrigid, liquidlike form of higher potential energy [Fig. 6(III)]. Finally, at high energies [Fig. 6(IV)] there are strong, rapid fluctuations with no favored potential-energy levels, which reflects the loose, liquidlike structure of the cluster. The situation is quite different for the softer 7-1 potential, particularly in the region of total energy for which $\langle U^* \rangle_s$ has a bimodal distribution (see Fig. 5). In this case [Figs. 7(B)–7(E)], the two ''modal'' values of $\langle U^* \rangle_s$ are close together and $\langle U^* \rangle_s$ never remains close to either for any considerable time, which precludes definition of a ''coexistence region'' in which the cluster exhibits different phases. In other words, when the pair potential is very soft and the total energy is in the bimodal region, the cluster performs transitions between isomers that are very close in energy and the time spent in each is too short to establish the properties of a quasistable phase.

Graphs of $\delta(E^*)$ showing two abrupt increases have been obtained recently by Krissinel and Jellinek [8] for Ni_{13} and Al_{13} using Gupta-like potentials. In the light of the results of the present paper, these findings may be attributed to the softness of the repulsive core of the potentials rather than to their many-body character. The same may probably also be said of the premelting phenomenon observed in transition-metal clusters described by Gupta-like and embedded-atom potentials when cluster size is one more than that of a complete (poly)icosahedron [3,4]. Because this latter effect has not been observed in LJ clusters, it has been attributed to the many-body character of the metallic cohesion. However, Fig. 8 shows that a 14-particle cluster with a soft-core (7-1) pair potential does exhibit two abrupt changes in $\delta(E^*)$, the first occurring at an energy well below the melting energy. This premelting effect arises from the destabilization of the extra atom that occurs before the melting of the cluster.
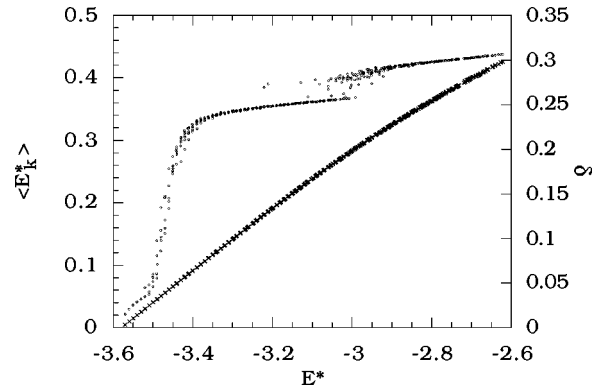
IV. SUMMARY AND CONCLUSIONS

Previous studies have shown that the cluster melting transition is dependent on the range of the attractive tail of the interatomic potential. In this work we have shown that the softness of the repulsive core of the potential also has a profound effect on cluster melting. Although the specific-heat curves of the 13-atom clusters studied all show a single peak corresponding to a well-defined cluster melting transition, their $\delta(E^*)$ curves show two distinct structural transitions: a low-energy transition at the onset of isomerizations involving only surface atoms and a second, higher-energy transition corresponding to the onset of isomerizations that also involve the central particle of the cluster. The second structural transition occurs at energies just below the cluster melting transition. Such behavior has been seen previously in studies of metal clusters, but in this case is not attributable to any many-body interaction. The two-step melting process is more evident the softer the core interaction. It was also found that 14-particle clusters with soft-core pair interactions exhibited premelting, another phenomenon that has been observed previously only in studies of metal clusters.

For all the potentials considered in this paper, the short-time-averaged potential energy of the 13-particle cluster has a bimodal distribution at total energies between those at which the long-time-averaged caloric curve changes slope. However, it is only for the potentials with relatively hard cores that the two modal potential-energy levels correspond to distinct quasistable phases between which the cluster fluctuates; when the core is soft, the modal potential-energy levels are close together and the cluster fluctuates too rapidly between them for it to be possible to consider either as a quasistable phase.

[1] C. Rey, L. J. Gallego, J. García-Rodeja, J. A. Alonso, and M. P. Iñiguez, Phys. Rev. B **48**, 8253 (1993).

[2] M. J. Grimson, Chem. Phys. Lett. **195**, 92 (1992).

[3] J. Jellinek and I. L. Garzón, Z. Phys. D **20**, 239 (1991).

[4] I. L. Garzón and J. Jellinek, in *Physics and Chemistry of Finite Systems: From Clusters to Crystals*, Vol. 374 of *NATO Advanced Study Institute, Series C: Mathematical and Physical Sciences*, edited by P. Jena, S. N. Khanna, and B. K. Rao (Kluwer, Dordrecht, 1992), p. 405; Z. B. Güvenç, J. Jellinek, and A. F. Voter, *ibid.,* p. 411.

[5] C. L. Briant and J. J. Burton, J. Chem. Phys. **63**, 2045 (1975).

[6] H.-P. Cheng and R. S. Berry, Phys. Rev. A **45**, 7969 (1992).

[7] F. Calvo and P. Labastie, Chem. Phys. Lett. **258**, 233 (1996).

[8] E. B. Krissinel and J. Jellinek, Int. J. Quantum Chem. **62**, 185 (1997).

[9] C. Rey and L. J. Gallego, Phys. Rev. E **53**, 2480 (1996).

[10] J. P. K. Doye and D. J. Wales, Science **271**, 484 (1996).

[11] M. H. J. Hagen and D. Frenkel, J. Chem. Phys. **101**, 4093 (1994).

[12] C. Rey, L. J. Gallego, and J. A. Alonso, Phys. Rev. B **49**, 8491 (1994).

[13] A. Cheng, M. L. Klein, and C. Caccamo, Phys. Rev. Lett. **71**, 1200 (1993).

[14] J. D. Weeks, D. Chandler, and H. C. Andersen, J. Chem. Phys. **54**, 5237 (1971).

[15] J. Jellinek, T. L. Beck, and R. S. Berry, J. Chem. Phys. **84**, 2783 (1986).

[16] H. L. Davis, J. Jellinek, and R. S. Berry, J. Chem. Phys. **86**, 6456 (1987).

[17] M. P. Allen and D. J. Tildesley, *Computer Simulation of Liquids* (Oxford University Press, Oxford, 1990).

[18] I. L. Garzón, M. Avalos-Borja, and E. Blaisten-Barojas, Phys. Rev. B **40**, 4749 (1989).

[19] S. Sugano, *Microcluster Physics* (Springer-Verlag, Berlin, 1991).